

Preparation, optimization, and in-vitro evaluation of aspirin/PEG solid dispersions using subcritical CO₂ by response surface methodology

Hossein Rostamian*, Mohammad Nader Lotfollahi^{*,†}, and Ali Mohammadi^{**}

*Faculty of Chemical, Petroleum and Gas Engineering, Semnan University, Semnan 35196-45399, Iran

**Department of Drug and Food Control, Faculty of Pharmacy, Tehran University of Medical Sciences, Tehran, Iran

(Received 3 May 2020 • Revised 7 July 2020 • Accepted 11 July 2020)

Abstract—This study reports on the preparation, optimization, and in vitro evaluation of micronized solid dispersions containing Polyethylene Glycol 4000 (PEG4000) and aspirin to increase the dissolution rate of aspirin in water. To achieve this goal, aspirin/PEG4000 composites were prepared and characterized by applying a solid dispersion method with subcritical CO₂. Employing response surface methodology (RSM) using the Box-Behnken design (BBD), the effects of different variables including pressure, concentration, drug/polymer ratio, and their interactions on drug content and yield of production were investigated. The closeness between the measured and predicted responses with $R^2 > 0.99$ demonstrated the validity of the statistical analysis. The optimal formulation obtained from RSM is at a pressure of 63.5 bar, concentration of 0.17 g/g_{Solution}, and drug/polymer ratio of 1. Under the optimized condition, the yield of production and drug content % reached 91.5% and 54.5%, respectively. Dissolution tests carried out in buffer phosphate solution at pH 7.4 showed a significant improvement in dissolution rate, with a rate approximately seven times faster than unprocessed aspirin. In addition, the in vitro drug release profile of produced composites showed an initial burst release of more than 80% in the first 2 min.

Keywords: Aspirin, Solid Dispersion, Dissolution Rate, Box-behnken Design, Subcritical CO₂

INTRODUCTION

Aspirin is a pain killer, analgesic, antipyretic, and anti-inflammatory drug [1,2]. Aspirin, which reduces inflammation, has a prophylactic effect on reducing the risk of cardiovascular events [3]. The stomach and upper intestine can absorb aspirin whose oral bioavailability and half-life are 40-50% and 15-20 min, respectively. Since aspirin should be transformed by the extensive hydrolysis in the gut and liver into salicylic acid, high and frequent dosing of this drug is needed. Thus, the bioavailability of aspirin as a poorly water-soluble drug should be improved [4].

The drugs with low solubility of their active pharmaceutical ingredients (API) have significant limitations to their bioavailability [5]. Most of the active compounds do not have a suitable dissolution rate and solubility in aqueous media. These types of drugs are classified as Class II APIs by the Biopharmaceutics Classification System (BCS). The dissolution rate of a drug can be improved by several techniques, such as micronization, pH adjustment, and the production of a composite by using the water-soluble polymers [5-11]. Among the various existing methods, the solid dispersion method is known as an effective way to improve the solubility and dissolution rate of poorly water-soluble drugs [12]. In the solid dispersion method, where active compounds are dispersed in a carrier matrix, there is an amorphous drug within a polymeric carrier, which results in an enhancement of the dissolution rate, absorption, and drug effectiveness [13,14]. The dissolu-

tion rate of solid dispersion can be also improved through the reduction of particle size, improving the wettability, avoidance of drug recrystallization, solubilization effect of polymer, and production of amorphous forms of the drugs [12,15]. The characteristics and concentration of the polymer affect the dissolution rate of drugs [16]. For this purpose, the polymer should be non-toxic and biodegradable with pharmaceutical usages. For instance, Polyethylene Glycol (PEG) can be used as a suitable carrier. PEG has been known as a common non-ionic hydrophilic polymer that reduces the aggregation of particles [17,18].

Conventional techniques, such as solvent evaporation, hot melt, and spray drying methods, are used for producing solid dispersions to improve the dissolution rate of drugs. These techniques have some limitations, such as thermal degradation of drug, low yield, and high amount of residual solvent. Methods utilizing sub- and supercritical fluids (SCFs) are used as the alternative methods having several advantages including the decrease in the mean particle size with low residual organic solvent content. The supercritical fluids exhibit interesting characteristics, such as high diffusivity approaching those of a gas, and high density and solvating properties that approach those of a liquid. Also, the properties of solvent power and selectivity (SCFs) can be easily adjusted by altering the temperature and pressure. These characteristics make them preferred fluids in various applications, especially in extraction, chemical synthesis, purification, particle formation, and polymerization [19,20]. They are widely applied in the pharmaceutical industry for applications such as micronization, particle coating, encapsulation, and improvement of dissolution rate of poorly water-soluble drugs [21,22]. Moreover, by using SCF the polymorphic purity and particle morphology can be controlled [5,23].

[†]To whom correspondence should be addressed.

E-mail: mnlotfollahi@semnan.ac.ir

Copyright by The Korean Institute of Chemical Engineers.

Carbon dioxide as one of the most applicable SCFs has moderate critical conditions, and it is non-toxic, non-flammable, low cost and easy to handle [24]. In addition, it is suitable for pharmaceutical processes that are heat-sensitive and should be contaminant-free [25]. Thus, it is appropriate to treat the active ingredients of drugs by the SCF technique [13]. CO₂ is applied as a solvent, co-solvent, anti-solvent, and cooling agent in different SCF processes such as rapid expansion of supercritical solution (RESS), gas anti-Solvent (GAS), supercritical anti-Solvent (SAS), particles from the gas-saturated solutions (PGSS), and pressure reduction of gas-expanded liquid (PPRGEL) methods [26,27].

In recent decades, many studies have been conducted to improve the dissolution rate of different types of drugs by using micronization and solid dispersion method with sub- and supercritical CO₂. Badens et al. [5] improved the dissolution of oxeiglitar by spray-freezing and supercritical anti-solvent. They investigated the various parameters such as particle size, flow properties, particle morphology, crystallinity, and precipitation yield for different formulations and showed that both methods exhibited an enhancement in the dissolution rates. Rostamian and Lotfollahi [28] used (RESS-SC) method to produce ultra-fine aspirin in the range of 0.17-6.61 μm. They investigated the influence of expansion pressure, pre-expansion temperature, spray distance, nozzle types, and nozzle diameter on the morphology and particle size of aspirin. They did not report the yield of production due to the low yield of RESS-SC method. Jafari et al. [1] applied GAS process to produce micronized pure aspirin. They studied the effects of solute concentration, solvent type, temperature, and the rate of anti-solvent addition on morphology and particle size of aspirin. By this technique, they produced aspirin microparticles with a mean size between 46 and 124 μm, but they did not report the yield of production. Also, they did not perform the dissolution study. Mondal et al. [29] applied subcritical CO₂ through PPRGEL method to produce micro- and nano-particles. They also proposed a thermodynamic model to calculate the time-variant reduction of the CO₂ pressure in gas expanded solution for the CO₂-acetone-cholesterol system. Their results showed that a large temperature drop was the dominant phenomenon. Prasad et al. [30] used subcritical CO₂ to produce ultra-fine particles of curcumin from acetone solution. They concluded that the precipitation of ultrafine particles of curcumin by PPRGEL method improved their bioavailability and hence the dissolution rates of particles. They also investigated the effect of initial pressure

and additives. To increase the bioavailability of silymarin, Yang et al. [14] applied solid dispersion method using solution-enhanced dispersion by supercritical fluids (SEDS). They studied the particle size, stability, and the value of the residual solvent of the product produced with SEDS and solvent evaporation. They utilized polyvinyl pyrrolidone K17 with a 1:5 ratio of silymarin to the polymer. The results of the in vitro and in vivo evaluations showed that silymarin solid dispersion produced by SEDS has no loss of silymarin after storage for six months, negligible residual solvent, and improvement of the oral absorption. Adeli [31] increased the bioavailability of azithromycin by solid dispersion using various PEG by the solvent evaporation method. They reported that the solubility and the dissolution rate of azithromycin were considerably improved by hydrophilic carriers, especially PEG6000. Vinjamur et al. [32] used subcritical CO₂ in PPRGEL method for the encapsulation of silica and tartaric acid (TA) nanoparticles by using CO₂ expanded solution. They also developed a model to evaluate supersaturation ratio, nucleation rates, growth rates, and average sizes of precipitated particles.

The present study's aim was to produce the composites of aspirin/Polyethylene Glycol 4000 (PEG4000) by the solid dispersion method using CO₂-expanded solvent technique to overcome the problem associated with the low dissolution rate of aspirin. This method can produce particles by a sub- and near-critical CO₂ (40-70 bar) with proper yield% of production. In this method, CO₂ is applied as a cooling agent and anti-solvent. The purpose of this study was to identify suitable conditions in terms of yield and drug loading for production of solid dispersions of micronized aspirin/PEG4000 using RSM methodology. In addition, the dissolution rate of produced solid dispersion was compared with the original aspirin one. To the best of our knowledge, the preparation, optimization, and in vitro evaluation of aspirin/PEG4000 composites produced with compressed CO₂ have not been reported in the literature.

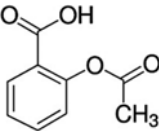
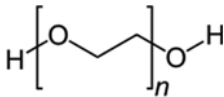
MATERIALS AND METHODS

In this section, first, the used materials are introduced. Then the experimental set-up and the procedure of experiments are explained. The analyses used for characterization of raw materials and the solid dispersion particles are elaborated in the section 2.4. Finally, the experimental design method based on the BBD is described.

1. Materials

Aspirin (C₉H₈O₄, >99%) and acetone as an organic solvent

Table 1. Some important physicochemical characteristics of aspirin and PEG4000 [33-35]

Name	Aspirin	PEG4000
Structure		
Physical state	White crystalline solid	White solid with a paraffin-like appearance
Molecular weight (g/mol)	180.16	3,500-4,500
Density (g/mL)	1.4 at 25 °C	1.2 g/mL at 20 °C
Melting point (°C)	136	53-58
Boiling point (°C)	140	270

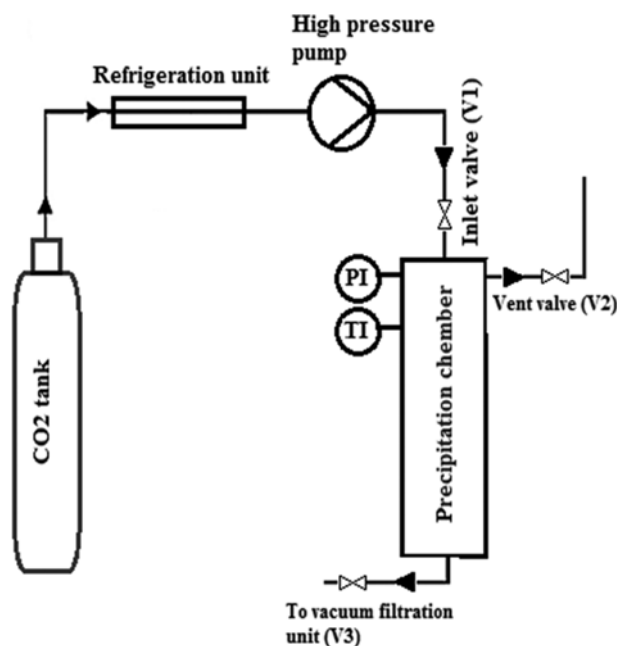


Fig. 1. Diagram of the set-up applied for the experiments.

(>99.5%) were purchased from Merck (Germany). Carbon dioxide (CO₂), applied as an anti-solvent and cooling agent, was prepared by the Air Product Company (UAE) with a purity of >99.99%. Table 1 shows some characteristics and structure of aspirin and PEG4000.

2. Experimental Set-up

The supercritical fluid extraction system was 101-300 AF (M), SITEC-Sieber Engineering Switzerland [36,37], utilized for solid dispersion process with subcritical CO₂. The experimental set-up demonstrated in Fig. 1 consisted of a refrigeration unit to liquefy CO₂, a pressure control valve (piston type air operated valve), and a metering pump (1.5 kW, LEWA). An inlet valve (V₁) carried the liquid CO₂ to the vessel, which is made of 316a stainless steel. The equilibrium vessel endures the pressure up to 300 bar, and its temperature was controlled with a thermostatic refrigerant bath up to 80 °C with an accuracy of ±0.5 °C. The V₂ valve was set on the top of the vessel to quickly decrease its pressure. The pipes, connectors, valves, and the equilibrium vessel were isolated to reduce the heat loss in the system.

3. Procedure of Experiments

In this study, the solid dispersion method based on the pressure reduction of gas-expanded solution process was applied to micronize aspirin/PEG4000 composites. First, the aspirin and PEG4000 were completely dissolved in acetone to prepare a homogeneous solution at predetermined mass ratios and concentrations. The experiment was carried out by loading the required amount of solution into the precipitation vessel. The vessel was then loaded with subcritical CO₂ at the pressure range of 45–65 bar. To run the experiments, the solution and injected CO₂ in the vessel were allowed to reach equilibrium at the desirable temperature and pressure. The required time for equilibrium was one hour, which was determined by performing some preliminary experiments. After achieving the equilibrium condition at the specific temperature and pressure, the pressure of the vessel was decreased to atmospheric

pressure during 50–75 sec. Thus, the temperature decrease of the solution resulted in precipitating the particles in the supersaturated solution. The rate of depressurization was kept constant at about 0.85±0.05 bar/sec for all the experiments. Then, a vacuum process in a microfiltration unit separated the particles from the bulk of the solution. These particles were gathered and analyzed to determine their size and morphology.

4. Characterization of Product

Microstructural analysis was studied by Philips XL30 Scanning electron microscopy (SEM). To analyze the SEM images, the particle size distribution (PSD) and the mean particle size were determined by counting about 100–150 particles arbitrarily chosen from the images.

The structure and phase of the product were studied by X-Ray diffraction (XRD) test using the Philips XRD analyzer with Co/Kα x-ray (40 kV and 30 mA). The data were recorded in the 2θ angle range of 5–80° with the defined step size of 0.02°.

Differential scanning calorimetry (DSC) thermograms were measured by a DSC system (model 500B; INUUNO, Inc., China) to define the thermal properties of the particles. Approximately, 4–5 mg of sample was located onto an alumina crucible. The temperature of the samples was increased from 25 to 150 °C with the rate of 10 °C/min under a nitrogen purge (50 mL/min).

The chemical structure of samples was also analyzed using Fourier-transform infrared spectroscopy (FTIR). FTIR studies for raw aspirin, raw PEG4000, and solid dispersion sample involved using

Table 2. Factors and their levels in the solid dispersion process

Factors	Symbols	Uncoded levels		
		-1	0	1
Pressure (bar)	P	45	55	65
Concentration (g/g _{Solution})	C	0.07	0.12	0.17
Mass drug/polymer ratio	Ratio	1	2.5	4

Table 3. BBD and the obtained drug content% (R1) and Yield% (R2) values

Runs	Pressure (bar)	Concentration (g/g _{Solution})	Ratio	Drug content % (R ₁)	Yield% (R ₂)
1	45	0.07	2.5	32.4	22.2
2	65	0.07	2.5	32.04	30.6
3	45	0.17	2.5	43.46	32.7
4	65	0.17	2.5	58.6	66.6
5	45	0.12	1	35.2	58.3
6	65	0.12	1	40.7	63.5
7	45	0.12	4	58.45	39.5
8	65	0.12	4	52.6	41.3
9	55	0.07	1	29.81	44.1
10	55	0.17	1	52.39	81.2
11	55	0.07	4	42.33	22.1
12	55	0.17	4	65.46	60.76
13	55	0.12	2.5	52.03	35
14	55	0.12	2.5	53.25	33.64
15	55	0.12	2.5	50.51	33.1

an FTIR spectrometer (FT-IR 8400S SHIMADZO, JAPAN) with a diamond-made reflector. Analyses were performed at scanning speed of 4 cm^{-1} and wave number range from 400 to $4,000\text{ cm}^{-1}$.

In vitro dissolution studies were performed using a magnetic stirrer in 200 mL of phosphate buffer solution (pH=7.4) at 37°C and stirring at 100 rpm. 25 mg of composite powder was intro-

duced into the dissolution medium. Samples of 2.0 mL were withdrawn after specific times and replaced by the equal volume of fresh medium. Afterward, at 265 nm, HALO DB-20 spectrophotometry was used to evaluate the concentration of drug in filtered aliquots versus time.

The content of aspirin in each composite was also determined

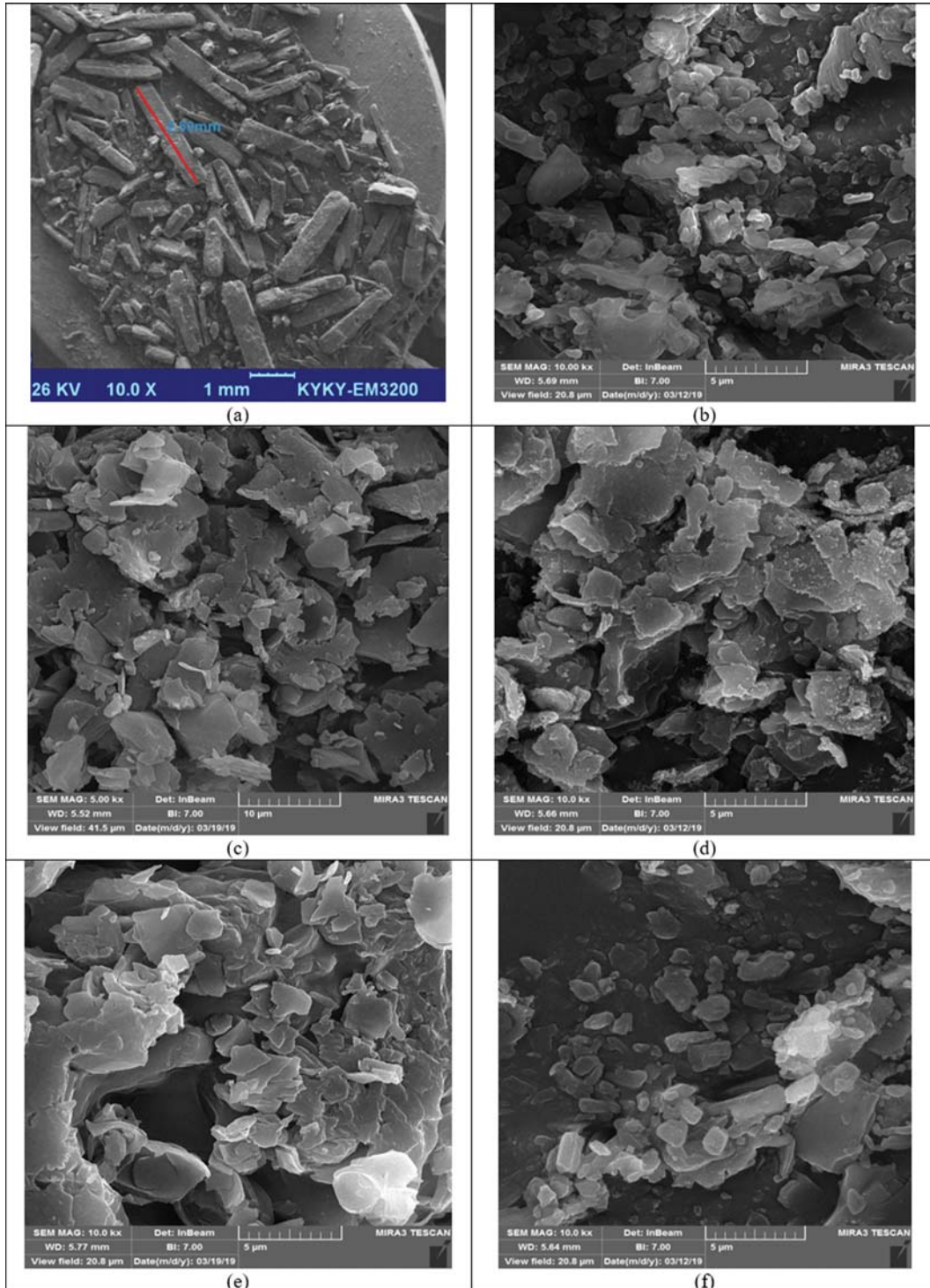


Fig. 2. Scanning electron microscopic images taken from (a) unprocessed aspirin and composites from (b) run #1, (c) run #2, (d) run #7, (e) run #12, and (f) run #14.

using a UV-visible spectrometer. An accurately weighed product was dissolved in 500 mL of phosphate buffer solution (pH=7.4). After complete dissolution, the mass of the drug in the prepared solution was measured via HALO DB-20 spectrometry at 265 nm. Then, the drug content was determined by Eq. (1):

$$\text{drug content\%} = \frac{\text{mass of drug in product}}{\text{total mass of product}} \times 100 \quad (1)$$

The yield of produced aspirin/PEG4000 composites was obtained by Eq. (2):

$$\text{Yield\%} = \frac{\text{mass of composite particles produced by solid dispersion method}}{\text{total initial mass of aspirin} + \text{PEG particles added to the formulation}} \times 100 \quad (2)$$

5. Experimental Design

To study the significance of the input parameters and recognize and optimize the interactions among them, Box-Behnken Design (BBD) according to the response surface methodology (RSM) was used. In the case of four variables, the experimental design of BBD is considered as a suitable statistical tool due to its fewer required runs than those of the central composite. The present study used a three-level BBD containing 15 runs to analyze the effects of various input parameters on the yield and the drug content. Input parameters were the operating pressure (45-65 bar), the drug concentration (0.07-0.17 g/g_{solution}), and the drug/polymer mass ratio (1:4). Furthermore, the drug content (e.g., the amount of drug in products) and yield were the responses of the model. Table 2 shows the applied ranges and levels in the experiments.

Analysis of variance (ANOVA) was applied for analyzing the obtained results. The second-order quadratic polynomial (Eq. (3)) is considered to model the responses as a function of the input parameters [35].

$$Y = \beta_0 + \sum \beta_i x_i + \sum \beta_{ii} x_i^2 + \sum \beta_{ij} x_i x_j \quad (3)$$

where, Y shows the response, x_i and x_j indicate the independent parameters. β_0 is a constant coefficient, and β_i , β_{ii} and β_{ij} stand for the respective coefficients of linear, quadratic, and interaction variables.

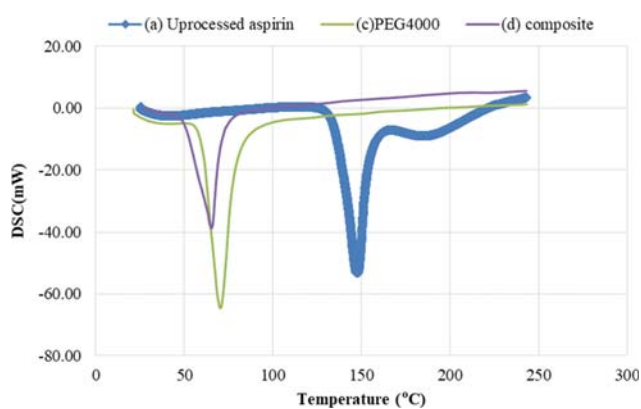


Fig. 3. Results of DSC test at temperature range of 25-250 °C at the presence of nitrogen gas at the flow rate of 50 mL/min for: (a) unprocessed aspirin, (b) PEG4000, and (c) aspirin/PEG4000 composite.

Table 3 demonstrates the BBD of experiments, including the input parameters and the responses of each experimental run. The number of experimental runs was 15. The Design-Expert Software can also be used to present the coefficients of the models, test the significance of the fitting, and determine the significance of the individual model coefficients.

RESULTS AND DISCUSSION

1. Characterization of the Aspirin/PEG4000 Composites

Fig. 2 indicates the images of SEM for the original aspirin and the products. One can observe in Fig. 2(a) that the unprocessed

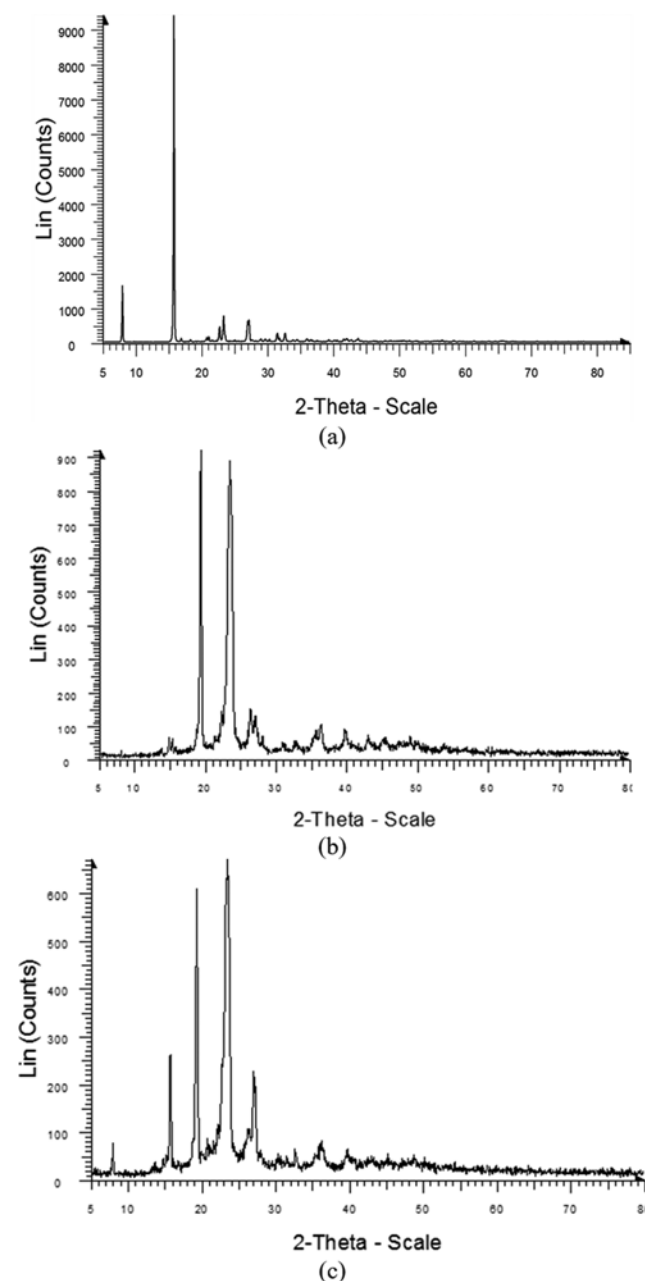
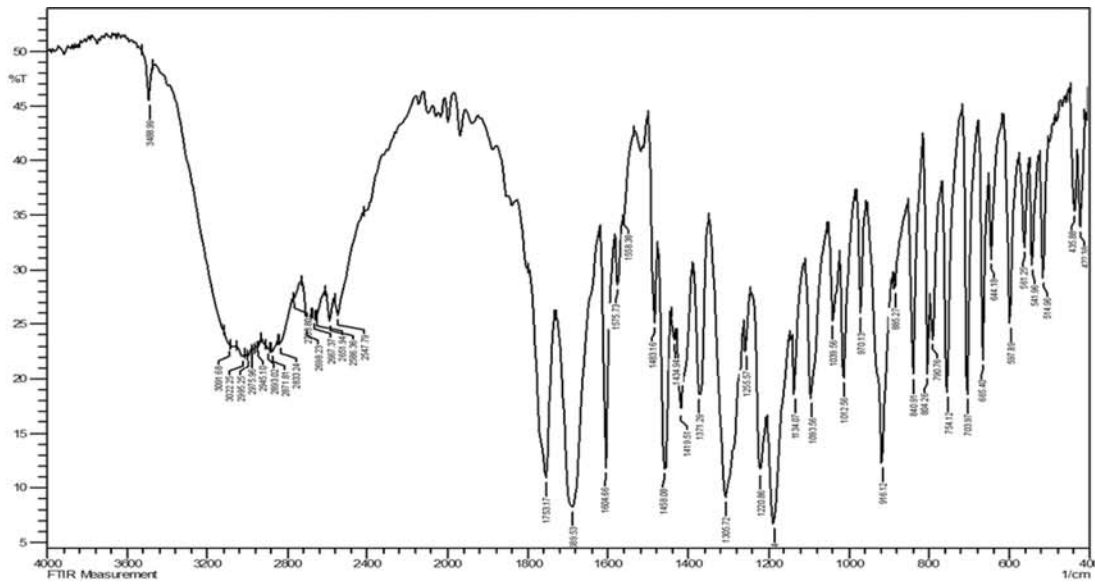
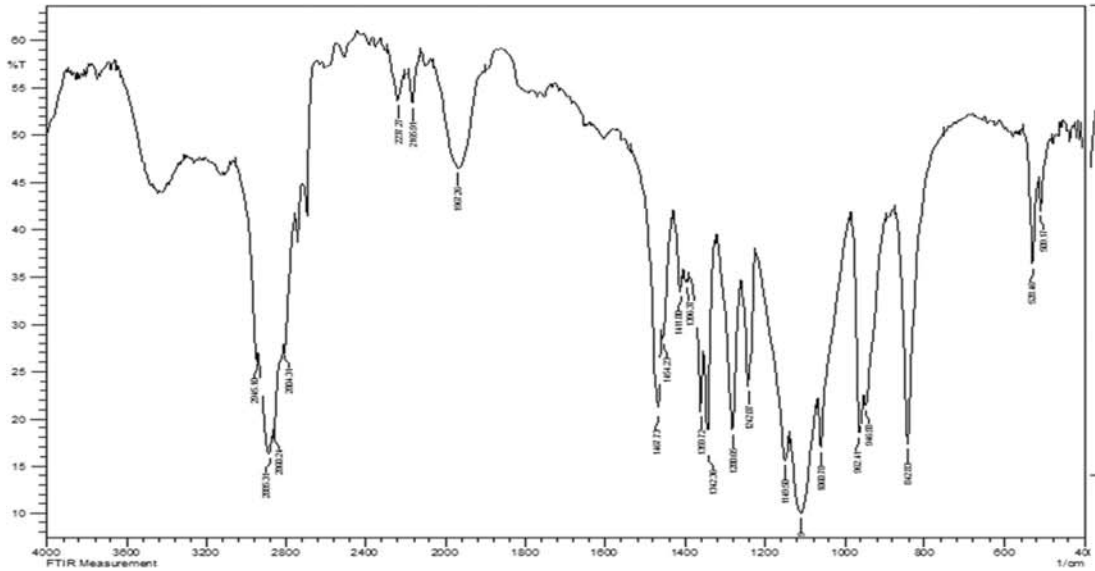


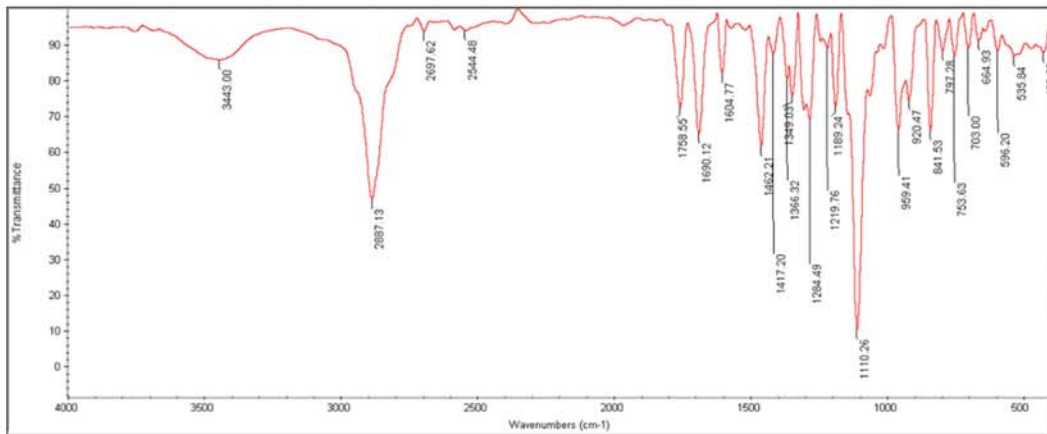
Fig. 4. Results of x-ray diffraction test, (a) unprocessed aspirin, (b) unprocessed PEG4000, and (c) composite of aspirin/PEG4000.



(a)



(b)



(c)

Fig. 5. Results of FTIR analysis for (a) the unprocessed aspirin, (b) PEG4000, and (c) the solid dispersion composite of Run #9.

aspirin has a rectangular morphology with a length of 465.7 ± 200 μm and a width of $1,160 \pm 636$ μm .

Fig. 2(b) to Fig. 2(f) report the SEM images of the composites made up of aspirin/PEG4000 with runs of #1, #2, #7, #12 and #14. Fig. 2 proves that the morphology of produced composites has irregular shape. Moreover, it can be concluded that the solid dispersion process can produce micronized composites, which are much smaller than the unprocessed aspirin.

Fig. 3 represents the DSC curves for the unprocessed aspirin, PEG4000, and the produced aspirin composite with the solid dispersion approach. The aspirin powder has a sharp endothermic peak at 147.8°C which corresponds to its melting point. The aspirin composite has a melting temperature of 65.2°C , near the melting temperature of PEG4000. Despite this observation, the endothermic peak of aspirin was not seen in solid dispersion composite prepared by the subcritical CO₂ approach. Such results show that aspirin was in a different phase (amorphous) in the aspirin/PEG composite [14,38].

Fig. 4 shows the results of the XRD tests conducted for the unprocessed aspirin, aspirin composite produced by the solid dispersion approach, and PEG4000. The main principal XRD peaks of aspirin ($2\theta=7.75$ and 15.6) exist in the XRD of composite. Additionally, the obtained results prove that the intensity of peaks for solid dispersion particles at specific 2θ points has been reduced compared to the unprocessed aspirin and PEG4000 particles. It is mainly owing to the reduction in the size of the particles. Moreover, a rough comparison between the pattern of XRD for unprocessed aspirin and produced composite can reveal the fact that aspirin content exists in the structure of composite because the main aspirin peaks are still located at XRD of composite. No other peaks exist rather than aspirin and PEG inside the pattern, showing the high purity of the aspirin composite.

Fig. 5 represents the FTIR analysis that belongs to the unprocessed aspirin, PEG4000, and the micronized composite of aspi-

rin/PEG4000 (Run #9). Note that there are no two compounds with different structures that produce the exact infrared spectrum, although some of the frequencies might be the same [39].

Fig. 5 also shows the principal peaks of aspirin at $1,183$, $1,688$, $1,604$, $1,305$, $1,755$, 925 , 754 , 703 , 665 , and $1,219$ cm^{-1} . They are indicated in both Fig. 5(a) and Fig. 5(c). The principal peaks of the aspirin and PEG4000 exist in the FTIR of composite (Fig. 5(c)). They are presented in Fig. 5(c), proving that the aspirin content is present in the composite structure.

In addition, Fig. 5 indicates that no significant changes on a molecular level or no undesirable chemical interaction between the drug and polymer have occurred. Although some minor structural perturbations may have occurred, the main peaks of the drug and polymer are clearly observed in the solid dispersion samples. This confirms that the investigated approach can produce aspirin without any change in the chemical structure of aspirin.

2. ANOVA Analysis

In this work, the accuracy and the significance of the developed RSM model were tested using the analysis of variance (ANOVA) [40]. ANOVA was carried out by applying Design-Expert software (Ver. 7.0.0). Fisher's test (F-test), probability (p-value), and variation coefficient (R-square) were applied for the evaluation of the reliability of the applied models [41].

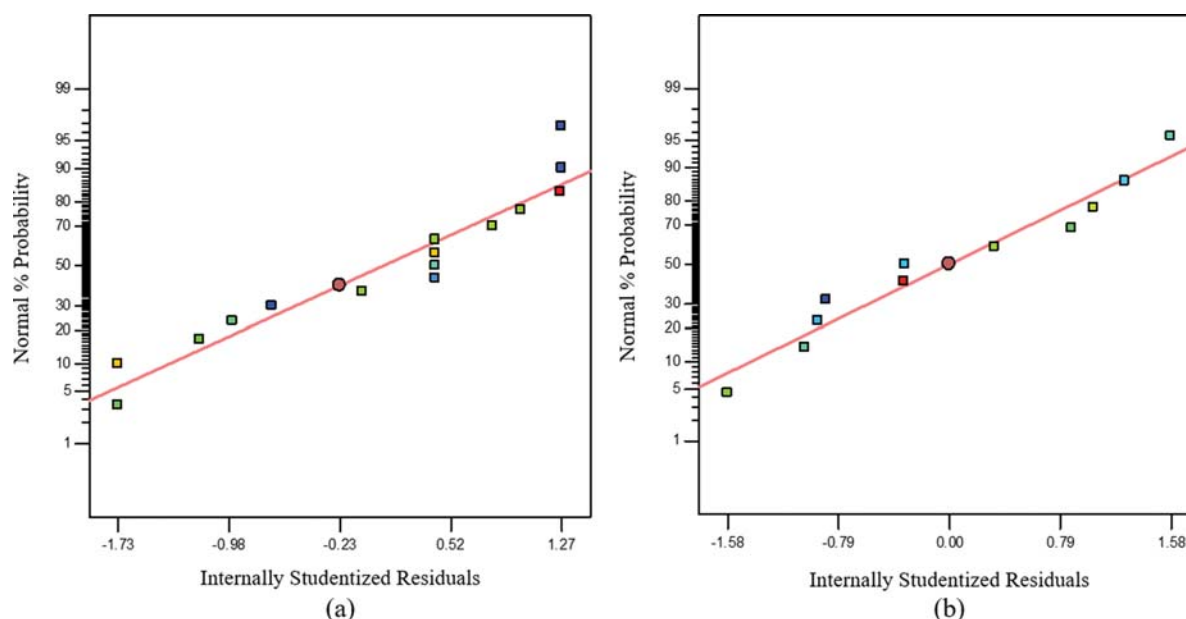
Table 4 and Table 5 report the statistical results obtained for the analysis of the aspirin/PEG4000 composite production using the ANOVA method for the drug content and yield of production, respectively. The present model F-value is 74.71 (Table 4). This result proves the significance of the model. The values of "Prob>F" are less than 0.05 showing the significance of the terms in the model. Hence, in this model, B, C, AB, AC, A², B², and AB² can be considered as significant terms. The values of the p-value greater than 0.1 show that the terms of the model are not significant. Moreover, the lack of fit F-value of 1.54 proves that the lack of fit is not significant when compared with the pure error, showing the validity

Table 4. ANOVA of the drug content of aspirin/PEG4000 composite

Source model	Sum of squares	df	Mean square	F-value	p-Value	
Model	1,674.586	9	186.0651	74.71134	<0.0001	Significant
A	0.030625	1	0.030625	0.012297	0.9160	
B	867.9861	1	867.9861	348.5253	<0.0001	
C	163.712	1	163.712	65.73582	0.0005	
AB	60.0625	1	60.0625	24.11709	0.0044	
AC	32.20563	1	32.20563	12.93163	0.0156	
A ²	114.7663	1	114.7663	46.08251	0.0011	
B ²	85.52915	1	85.52915	34.3428	0.0021	
A ² C	11.4242	1	11.4242	4.587196	0.0851	
AB ²	28.61461	1	28.61461	11.48972	0.0195	
Residual	12.45227	5	2.490454			
Lack of fit	8.683468	3	2.894489	1.536027	0.4177	Not significant
Pure error	3.7688	2	1.8844			
Cor total	1,687.038	14				
Std. dev.	1.58		R-squared	0.9926		
Mean	46.62		Adj. R-squared	0.9793		
C.V. %	3.39		AdEquation precision	26.098		

Table 5. ANOVA of the yield of production of aspirin/PEG4000 composite

Source model	Sum of squares	df	Mean square	F-value	p-Value	
Model	4,349.94	9	483.3269	425.8637	<0.0001	Significant
A	12.25	1	12.25	10.79359	0.0218	
B	14,34.894	1	1,434.894	1264.298	<0.0001	
C	870.2792	1	870.2792	766.8109	<0.0001	
AB	162.5625	1	162.5625	143.2353	<0.0001	
A ²	6.837664	1	6.837664	6.024728	0.0576	
B ²	27.94	1	27.94	24.61819	0.0042	
C ²	872.9215	1	872.9215	769.139	<0.0001	
A ² B	107.0185	1	107.0185	94.29492	0.0002	
AB ²	155.7613	1	155.7613	137.2426	<0.0001	
Residual	5.674667	5	1.134933			
Lack of fit	3.7576	3	1.252533	1.306719	0.4612	Not significant
Pure error	1.917067	2	0.958533			
Cor total	4,355.617	14				
Std. dev.	1.07		R-squared	0.9987		
Mean	44.31		Adj R-squared	0.9964		
C.V. %	2.4		Adeq precision	68.070		

**Fig. 6. Normal probability plot of (a) drug content (R1) and (b) yield (R2).**

of the model [42]. According to the results in Table 4, the amounts of R^2 and R^2 -adj are 0.9926 and 0.9793, respectively. Therefore, the predicted results are in logical agreement with the experimental data.

According to Table 5, the model's F-value of 425.86 proves that the performance of the model for the yield of production of aspirin/PEG4000 composite is significant. One can see that the parameters of A, B, C, AB, A², B², C², A²B, AB² are the main terms of the applied model. The lack of fit F-value of 1.31 shows its insignificance in comparison with the pure error. The adEquation precision of 68.07 represents an adequate signal. The values of R^2 and R^2 -adj are 0.9987 and 0.9964, respectively. These results show that the experimental data agree well with the predictions.

3. Residual Analysis and Model Checking

In this work, the accuracy of assumptions, including normality, constant error, and completely randomized design were confirmed by testing the residuals [38,43]. Plotting the normal probability of the studentized residuals is an essential diagnostic plot. Fig. 6 indicates the percentage of the normal probability in terms of internally studentized residuals for the yield and drug content responses, respectively. The normal probability plot reveals that the residuals have a normal distribution the points of which are in a straight-line arrangement.

4. Proposed Models

Eq. (4) shows the third-order polynomial model versus code

factors, including pressure (A), concentration (B), and the mass ratio of drug/polymer (C). The model estimates the drug content of aspirin/PEG4000 composites as a response.

$$\begin{aligned} \text{Drug content} = & +52.14 - 0.088 * A + 10.42 * B + 6.40 * C \\ & + 3.88 * A * B - 2.84 * A * C - 5.5 * A^2 \\ & - 4.80 * B^2 + 2.39 * A^2 * C + 3.78 * A * B^2 \end{aligned} \quad (4)$$

In Eq. (4), the coefficients show the specific weight for each variable of the model, while the signs contain synergistic (+) and antagonistic (-) influences of the parameters on the response. Fig. 7

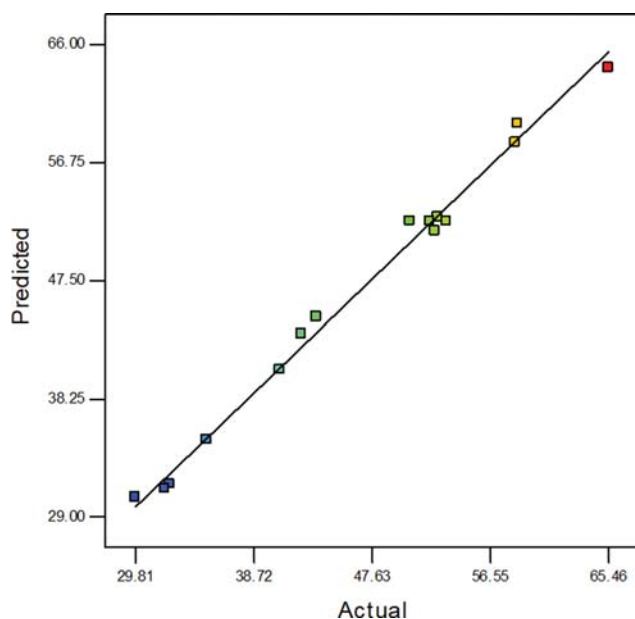


Fig. 7. Comparison between experimental (actual) and predicted values of drug content of composites.

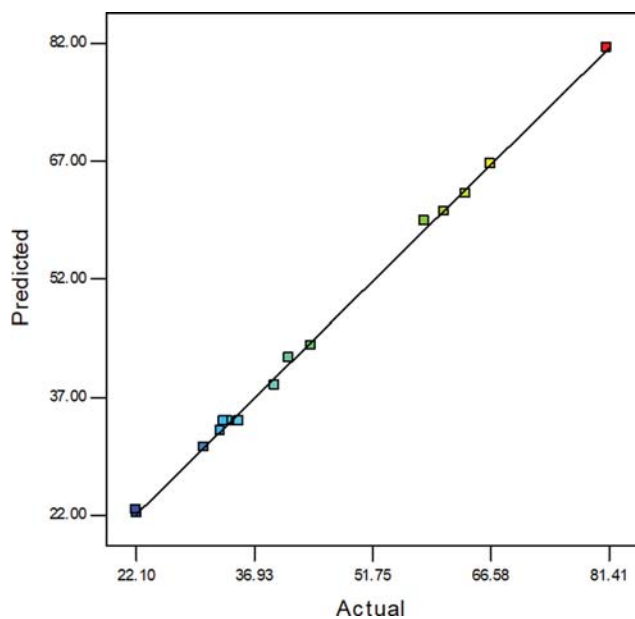


Fig. 8. Comparison between experimental (actual) and predicted values of yield of solid dispersion process.

presents the predicted amounts of response in terms of the actual response value of the drug content. The data points around the 45° line show the excellent fit of the present model.

Eq. (5) shows the final version of the empirical model versus code factors to estimate the yield of the solid dispersion process in the case of production of the aspirin/PEG4000 composites as a response.

$$\begin{aligned} \text{Yield} = & +33.91 + 1.75 * A + 18.94 * B - 10.43 * C \\ & + 6.38 * A * B + 1.36 * A^2 + 2.75 * B^2 \\ & + 15.38 * C^2 - 7.32 * A^2 * B + 8.82 * A * B^2 \end{aligned} \quad (5)$$

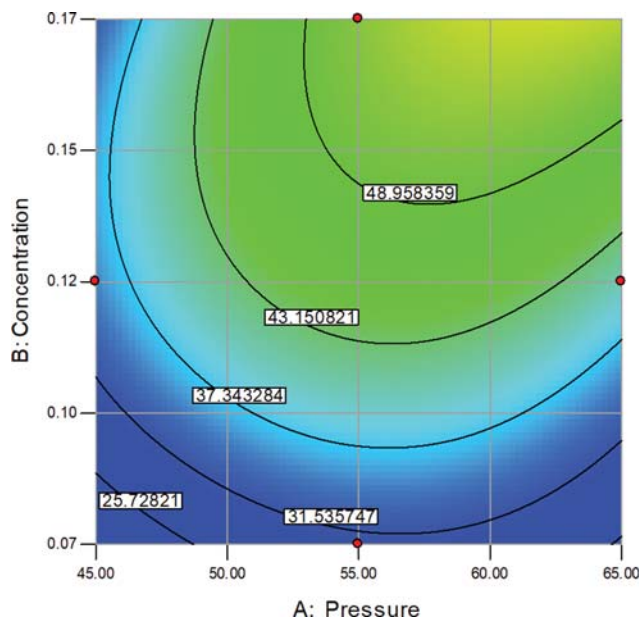


Fig. 9. The contour plot for the interaction effect of pressure (A) and concentration (B) on the drug content of aspirin/PEG4000 composites.

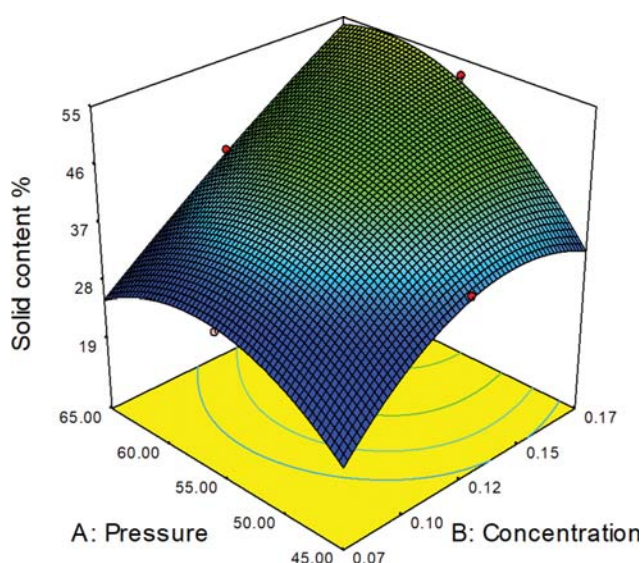


Fig. 10. The 3-D surface for the interaction effect of pressure (A) and concentration (B) on drug content of aspirin/PEG4000 composites.

Fig. 8 compares the predicted amount of response in terms of actual response value for the yield of production. Fig. 8 demonstrates a satisfactory regress of the model just as Fig. 7 does.

5. Effects of Process Parameters

To determine how the yield and drug content of aspirin/PEG4000 composites are affected by the parameters of pressure, concentration, and the mass ratio of drug/polymer, several tests were conducted by pressures in the range of 45-65 bar, concentrations in the range of 0.07-0.17 g/g_{Solution}, and under various mass ratios of drug/polymer in the range of 1-4. Fig. 9 and Fig. 10 illustrate the 3D and the contour plots that show the interactive effect of pressure and concentration on drug content percent of aspirin/PEG4000 composites when the mass ratio is constant. In general, the percent of drug content increases when the concentration increases and the pressure increases. These figures clearly confirm that the percent of the drug content increases up to a specific limit at any fixed concentration by increasing the pressure. Then, it has almost a fixed value. Moreover, these figures prove that the ascending trend of the drug content in terms of concentration is more determining when higher levels of pressure exist. In addition, based on Fig. 10, the concentration trend shows a maximum point at low pressure. This effect can be attributed mainly to the increase in the available solute species (subsequently, an increase in the degree of supersaturation and concentration gradient) for the growth of the nuclei produced in the bulk solution. High concentration gradient and supersaturation lead to the aspirin precipitation; therefore, a higher percentage of drug content is produced.

The interactive effect of pressure and mass ratio on the percent of drug content of aspirin/PEG4000 composites is shown in Fig. 11. It was found that the percent of drug content increases when the mass ratio of drug/polymer composite increases. Generally, the increasing trend of drug content in the terms of mass ratio is more determining when lower levels of pressure exist. Hence, at each

constant concentration, a lower mass ratio leads to a lower % drug content. The obtained results show that the content of polymer in the formulation (mass ratio of drug/polymer) significantly affects the drug precipitation.

Fig. 12 and Fig. 13 show the 3-D and contour plots for the interactive effect of the pressure and concentration on the yield of the produced aspirin/PEG composites. Based on these figures, the increasing trend of the yield versus concentration becomes more significant than cases in which pressure increases. Moreover, at a low level of concentration (0.07 g/g_{Solution}), the precipitation pressure does not significantly affect the yield of the products. In spite of this, when the concentration of the solution becomes higher (0.17 g/g_{Solution}), the percent of the yield is significantly affected by

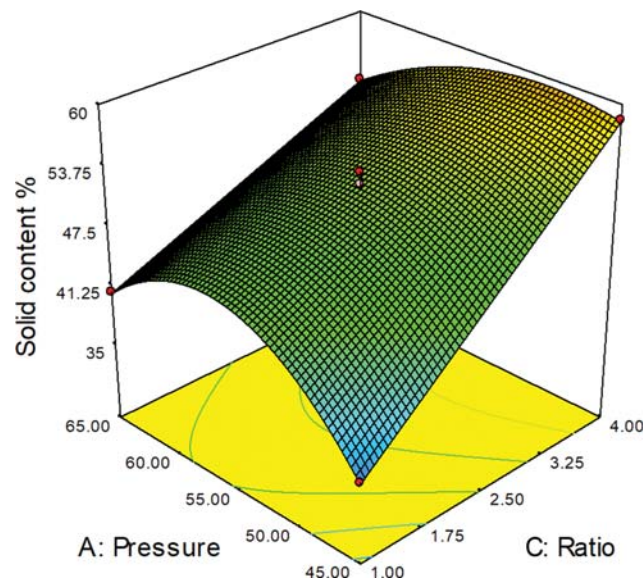


Fig. 11. The 3-D surface for the interaction effect of pressure (A) and mass ratio (C) on drug content of aspirin/PEG4000 composites.

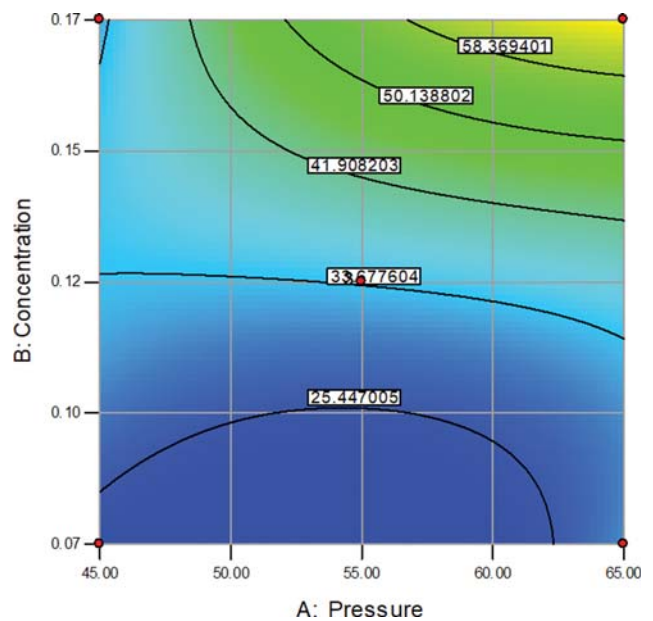


Fig. 12. The contour plot for the interaction effect of pressure (A) and concentration (B) on yield of production.

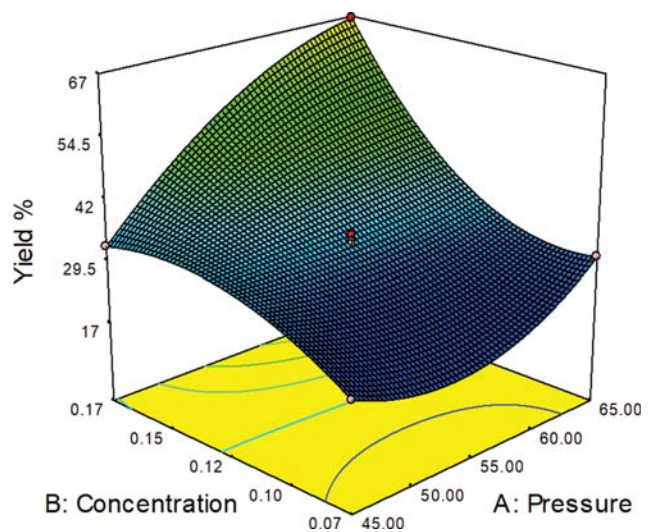


Fig. 13. The 3-D surface for the interaction effect of pressure (A) and concentration (B) on yield of production.

Table 6. The drug content % and yield % at the optimal condition that pressure is 63.5 bar, concentration is 0.17 and the drug/polymer ratio is 1

Response	Experimental value	Predicted value	AR _E %
Drug content %	57.9	54.47	5.92
Yield %	87.52	91.48	4.57

the pressure. These obtained results can be due to the degree of supersaturation and the nature of drug/polymer composites at various conditions.

This investigation's aim was to reach maximum yield and the highest possible percent of drug content. Table 6 reports the optimum values of the solid dispersion process in producing aspirin/PEG4000 composite. All three factors have limits on their lower and upper coded values. To recognize the accuracy of the predicted values, the absolute percent of the relative error (AR_E%) was computed based on Eq. (6):

$$AR_E\% = \frac{|X_{i,exp} - X_{i,calc}|}{X_{i,exp}} \times 100 \quad (6)$$

The optimization part of Design-Expert software indicated that the optimum condition of the operational pressure was 63.5 bar, the concentration was 0.17 g/g_{Solution} and the drug/polymer ratio was 1. Under the optimum condition, the yield percent can reach 91.48%, where the drug content is 54.47%. Based on the results reported in Table 6, the experimental and predicted values of the yield and drug content are close to each other. This result suggests that the optimized condition is reliable and rational.

6. In Vitro Dissolution Test

Fig. 14 presents the obtained results of the in vitro dissolution experiments conducted on the unprocessed aspirin and composites of aspirin/PEG4000 (Runs #1, #7, and #12). The 15% of the dissolved aspirin was obtained after 10 min for unprocessed aspirin. However, at this time, more than 90% of the aspirin was dissolved for composites of Runs #1, #7, and #12. Compared with the unprocessed aspirin, the enhanced dissolution of the composites is not only due to increasing the saturation solubility of the drug, but also to decreasing the size of the particles. Moreover, since the

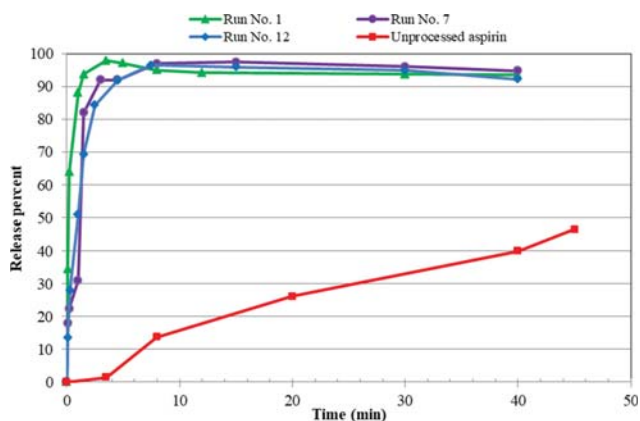


Fig. 14. In vitro dissolution profiles of unprocessed aspirin and different types of aspirin/PEG4000 composites.

evaporation of carbon dioxide takes place during the micronization process, the porosity of the microparticles can positively influence the dissolution of aspirin. Finally, the aspirin/PEG4000 composites have much higher dissolution rates than the unprocessed one.

CONCLUSION

The present investigation mainly focused on the preparation, optimization (i.e., maximum yield and the highest possible percent of drug content) and in vitro evaluation of micronized solid dispersions containing a hydrophilic carrier (PEG4000) and aspirin by design of experiments. The major influences of three factors, including pressure, concentration, and the mass ratio of drug to polymer on the responses and their interactions, were studied. The optimization proved that the pressure of 63.5 bar, the concentration of 0.17 g/g_{Solution} and mass ratio of 1 resulted in the simultaneous maximum yield and the highest possible content of the aspirin. It has been recognized that the results of the mathematical model are reliable when compared to the experimental values, and a predictive tool with excellent accuracy was proposed.

REFERENCES

1. D. Jafari, I. Yarneshad, S. M. Nowee and S. H. N. Baghban, *Ind. Eng. Chem. Res.*, **54**, 3685 (2015).
2. J. Phillips, *Physica A*, **415**, 538 (2014).
3. Y. Shi, A. Wan, Y. Shi, Y. Zhang and Y. Chen, *Biomed. Res. Int.*, **2014**, 6 (2014).
4. K. B. Deshpande and V. S. Mastiholmath, *Int. J. Pharm. Res.*, **5**, 12 (2013).
5. E. Badens, V. Majerik, G. Horváth, L. Szokonya, N. Bosc, E. Teilaud and G. Charbit, *Int. J. Pharm.*, **377**, 25 (2009).
6. M. Rahimi, P. Valeh-e-Sheyda and H. Rashidi, *Korean J. Chem. Eng.*, **34**(11), 3017 (2017).
7. K. Yuvaraja, S. K. Das and J. Khanam, *Korean J. Chem. Eng.*, **32**, 132 (2015).
8. K.-R. Kwon and S.-D. Yeo, *Korean J. Chem. Eng.*, **35**, 1860 (2018).
9. F. Zabihi, M. Yang, Y. Leng and Y. Zhao, *J. Supercrit. Fluids*, **99**, 15 (2015).
10. K. Diaf, Z. El Bahri, N. Chafi, L. Belarbi and A. Mesli, *Chem. Paper*, **66**, 779 (2012).
11. F. Sadeghi, M. Ashofteh, A. Homayouni, M. Abbaspour, A. Nokhodchi and H. A. Garekani, *Colloids Surf. B. Biointerfaces*, **147**, 258 (2016).
12. S. Bandari, S. Jadav, B. B. Eedara, R. Jukanti and P. R. Veerareddy, *Korean J. Chem. Eng.*, **30**, 238 (2013).
13. M. Rossmann, A. Braeuer and E. Schluecker, *J. Supercrit. Fluids*, **89**, 16 (2014).
14. G. Yang, Y. Zhao, N. Feng, Y. Zhang, Y. Liu and B. Dang, *Asian J. Pharm. Sci.*, **10**, 194 (2015).
15. S. Ferdosh, M. Z. I. Sarker, N. N. N. Ab Rahman, M. J. H. Akand, K. Ghafoor, M. B. Awang and M. O. Ab Kadir, *Korean J. Chem. Eng.*, **30**, 1466 (2013).
16. S. P. Chaudhari and R. P. Dugar, *J. Drug. Deliv. Sci. Tec.*, **41**, 68 (2017).

17. K. Knop, R. Hoogenboom, D. Fischer and U.S. Schubert, *Angew. Chem. Int. Ed. Engl.*, **49**, 6288 (2010).
18. K.-T. Kwon, M. S. Uddin, G.-W. Jung and B.-S. Chun, *Korean J. Chem. Eng.*, **28**, 2044 (2011).
19. J. S. Kim and H. Y. Jo, *Korean J. Chem. Eng.*, **37**, 1086 (2020).
20. G. Sodeifian, S. A. Sajadian, F. Razmimanesh and N. S. Ardestani, *Korean J. Chem. Eng.*, **35**(10), 2097 (2018).
21. I. L. Jung, S. Haam, G. Lim and J. H. Ryu, *Korean J. Chem. Eng.*, **28**(9), 1945 (2011).
22. M. Charoenchaitrakool, W. Trisilanun and P. Srinopakhun, *Korean J. Chem. Eng.*, **27**(3), 950 (2010).
23. S. M. Chitanvis, *Physica A*, **322**, 55 (2003).
24. C. N. Han and C. H. Kang, *Korean J. Chem. Eng.*, **34**(6), 1781 (2017).
25. Z. Huang, G.-B. Sun, Y. C. Chiew and S. Kawi, *Powder Technol.*, **160**, 127 (2005).
26. K. T. Kwon, M. S. Uddin, G. W. Jung and B. S. Chun, *Korean J. Chem. Eng.*, **28**(10), 2044 (2011).
27. C. Chinnarasu, A. Montes, C. Pereyra, L. Casas, M. T. Fernández-Ponce, C. Mantell and E. M. De la Ossa, *Korean J. Chem. Eng.*, **33**(2), 594 (2016).
28. H. Rostamian and M. N. Lotfollahi, *Part. Sci. Technol.*, **38**(5), 617 (2020).
29. M. Mondal, S. Roy and M. Mukhopadhyay, *Ind. Eng. Chem. Res.*, **54**(13), 3451 (2015).
30. R. Prasad, R. Patsariya and S. V. Dalvi, *Powder Technol.*, **310**, 143 (2017).
31. E. Adeli, *Braz. J. Pharm. Sci.*, **52**, 1 (2016).
32. M. Vinjamur, M. Javed and M. Mukhopadhyay, *J Supercrit. Fluids*, **79**, 216 (2013).
33. C. McLoughlin, W. McMinn and T. Magee, *Powder Technol.*, **134**, 40 (2003).
34. O. Corrigan, C. Murphy and R. Timoney, *Int. J. Pharm.*, **4**, 67 (1979).
35. P. Shrimal, G. Jadeja, J. Naik and S. Patel, *J. Drug Deliv. Sci. Tec.*, **53**, 101225 (2019).
36. H. Baseri, M. N. Lotfollahi and A. H. Asl, *J. Food Process. Eng.*, **34**, 293 (2011).
37. H. Baseri, A. Haghighi-Asl and M. N. Lotfollahi, *Chem. Eng. Technol.*, **33**, 267 (2010).
38. P. Dittanet, S. Phothipanyakun and M. Charoenchaitrakool, *J. Taiwan Inst. Chem. E.*, **63**, 17 (2016).
39. Z. Movasaghi, S. Rehman and D. I. Rehman, *Appl. Spectrosc. Rev.*, **43**(2), 134 (2008).
40. V. Bewick, L. Cheek and J. Ball, *Crit Care*, **7**(6), 451 (2003).
41. H. R. Lindman, *Analysis of variance in experimental design*, Springer Science & Business Media, New York (1992).
42. A. Dean, D. Voss and D. Draguljić, *Design and analysis of experiments*, Vol. 1. New York, Springer (1999).
43. N. Wichianphong and M. Charoenchaitrakool, *J. Ind. Eng. Chem.*, **62**, 375 (2018).